ZD6474 Inhibits Vascular Endothelial Growth Factor Signaling, Angiogenesis, and Tumor Growth following Oral Administration

Stephen R. Wedge,[1] Donald J. Ogilvie, Michael Dukes, Jane Kendrew, Rosemary Chester, Janet A. Jackson, Sarah J. Boffey, Paula J. Valentine, Jon O. Curwen, Helen L. Musgrove, George A. Graham, Gareth D. Hughes, Andrew P. Thomas, Elaine S. E. Stokes, Brenda Curry, Graham H. P. Richmond, Peter F. Wadsworth, Alison L. Bigley, and Laurent F. Hennequin

Departments of Cancer and Infection Research [S. R. W., D. J. O., M. D., J. K., R. C., J. A. J., S. J. B., P. J. V., J. O. C., H. L. M., G. A. G., G. D. H., A. P. T., E. S. E. S., B. C.] and Safety Assessment [G. H. P. R., P. F. W., A. L. B.], AstraZeneca, Cheshire SK10 4TG, United Kingdom, and AstraZeneca Pharma, Centre de Recherches, 51689 Reims Cedex 2, France [L. F. H.]

ABSTRACT

ZD6474 [N-(4-bromo-2-fluorophenyl)-6-methoxy-7-[(1-methylpiperidin-4-yl)methoxy]quinazolin-4-amine] is a potent, p.o. active, low molecular weight inhibitor of kinase insert domain-containing receptor [KDR/vascular endothelial growth factor receptor (VEGFR) 2] tyrosine kinase activity (IC_{50} = 40 nM). This compound has some additional activity *versus* the tyrosine kinase activity of fms-like tyrosine kinase 4 (VEGFR3; IC_{50} = 110 nM) and epidermal growth factor receptor (EGFR/HER1; IC_{50} = 500 nM) and yet demonstrates selectivity against a range of other tyrosine and serine-threonine kinases. The activity of ZD6474 *versus* KDR tyrosine kinase translates into potent inhibition of vascular endothelial growth factor-A (VEGF)-stimulated endothelial cell (human umbilical vein endothelial cell) proliferation *in vitro* (IC_{50} = 60 nM). Selective inhibition of VEGF signaling has been demonstrated *in vivo* in a growth factor-induced hypotension model in anesthetized rat: administration of ZD6474 (2.5 mg/kg, i.v.) reversed a hypotensive change induced by VEGF (by 63%) but did not significantly affect that induced by basic fibroblast growth factor. Once-daily oral administration of ZD6474 to growing rats for 14 days produced a dose-dependent increase in the femoro-tibial epiphyseal growth plate zone of hypertrophy, which is consistent with inhibition of VEGF signaling and angiogenesis *in vivo*. Administration of 50 mg/kg/day ZD6474 (once-daily, p.o.) to athymic mice with intradermally implanted A549 tumor cells also inhibited tumor-induced neovascularization significantly (63% inhibition after 5 days; $P < 0.001$). Oral administration of ZD6474 to athymic mice bearing established (0.15–0.47 cm^3), histologically distinct (lung, prostate, breast, ovarian, colon, or vulval) human tumor xenografts or after implantation of aggressive syngeneic rodent tumors (lung, melanoma) in immunocompetent mice, produced a dose-dependent inhibition of tumor growth in all cases. Statistically significant antitumor activity was evident in each model with at least 25 mg/kg ZD6474 once daily ($P < 0.05$, one-tailed *t* test). Histological analysis of Calu-6 tumors treated with 50 mg/kg/day ZD6474 for 24 days showed a significant reduction (>70%) in CD31 (endothelial cell) staining in nonnecrotic regions. ZD6474 also restrained growth of much larger (0.9 cm^3 volume) Calu-6 lung tumor xenografts and induced profound regression in established PC-3 prostate tumors of 1.4 cm^3 volume. ZD6474 is currently in Phase I clinical development as a once-daily oral therapy in patients with advanced cancer.

INTRODUCTION

VEGF[2] is a key stimulus for vasculogenesis and angiogenesis. This cytokine induces a vascular sprouting phenotype by inducing endothelial cell proliferation, protease expression, and migration and subsequent organization of cells to form a capillary tube (1–3). VEGF also asserts a role in many related aspects of vascular growth and remodeling, including the mobilization and differentiation of bone marrow-derived endothelial cell progenitors (4, 5), intussusception (6), endothelial cell survival signaling in newly formed vasculature (7, 8), and the recruitment of mural cells to facilitate vessel stabilization (9, 10). In addition, VEGF induces significant vascular permeability (11, 12), promoting formation of a hyperpermeable, immature vascular network that is characteristic of pathological angiogenesis.

Although a wide range of angiogenic stimulators and inhibitors have been identified (see Ref. 13 for review), inhibition of VEGF signal transduction alone may represent a particularly attractive therapeutic approach, given its pivotal role in pathological angiogenesis, including the sustained neovascularization required to support tumor growth and metastasis (14). Such a strategy is reliant on low endothelial cell turnover in the adult, with angiogenesis being predominantly confined to ovarian endocrine function (15) and wound healing (16). In the normal quiescent state, vessels are stabilized by periendothelial support and signaling from angiopoietin-1/Tie-2 (17) and potentially Ephrin B2/EphB4 (18) ligand/receptor complexes. In contrast, VEGFRs are up-regulated on endothelium at sites of active angiogenesis (19), providing an opportunity for selective therapeutic intervention. Furthermore, VEGF overexpression by tumor cells occurs frequently in response to hypoxia (20, 21), loss of tumor suppressor gene function (22, 23), and oncogene activation (24, 25). The enhanced vascular permeability induced by VEGF in this setting may also increase tumor nutrient and catabolite exchange as well as facilitate the extravasation of macromolecular proteins (thereby promoting development of a tumor stroma) and intravasation of tumor cells. Consequently, it is hypothesized that inhibition of VEGF signaling will provide a means for stabilizing or slowing the progression of solid tumor disease.

There are three associated transmembrane receptors for vascular endothelial growth factor family ligands found on endothelium, Flt-1 (VEGFR1), KDR (VEGFR2), and Flt-4 (VEGFR3), which are related to the PDGFR family (26). Each receptor possesses intrinsic tyrosine kinase activity that is stimulated after ligand binding and receptor dimerization and is mandatory for transmission of a cytoplasmic signaling response. Flt-1 and KDR have different binding specificities for the separate isoforms of VEGF (generated by alternative exon splicing) and for additional vascular endothelial growth factor family members (PlGF and VEGF-B, -C, and -D) that can also be subjected to alternative exon splicing or proteolytic processing (see Ref. 27 for review). Flt-4 only binds VEGF-C and -D and is largely located on

[1] To whom requests for reprints should be addressed, at Cancer and Infection Research, AstraZeneca, Mereside, Alderley Park, Macclesfield, Cheshire SK10 4TG, United Kingdom. Phone: 44-1625-513236; Fax: 44-1625-513624; E-mail: steve.wedge@astrazeneca.com.

[2] The abbreviations used are: VEGF, vascular endothelial growth factor-A; bFGF, basic fibroblast growth factor; KDR, kinase insert domain-containing receptor; Flt, fms-like tyrosine kinase; EGFR, epidermal growth factor receptor; PDGFR, platelet-derived growth factor receptor; Tie-2, tunica interna endothelial cell kinase; FGFR1, fibroblast growth factor receptor 1; IGF-1R, insulin-like growth factor 1 receptor; MAPK, mitogen-activated protein kinase; MEK, MAPK kinase; FAK, focal adhesion kinase; CDK2, cyclin-dependent kinase 2; PDK1, phosphoinositide-dependent kinase 1; HUVEC, human umbilical vein endothelial cell; TKI, tyrosine kinase inhibitor; VEGFR, vascular endothelial growth factor receptor; EGF, epidermal growth factor; TUNEL, terminal deoxynucleotidyl transferase-mediated nick end labeling.

lymphatic endothelium (28–30). Clearly, there is a range of potential signaling responses that may be mediated through these receptors, particularly when one considers the potential for receptor homo- and heterodimerization (31). In addition, some isoforms of VEGF have been shown recently to bind to neuropilin 1 and 2 coreceptors on endothelial and tumor cells, and these coreceptors were found to cooperate with Flt-1 and KDR, although the biological significance of these interactions remains to be fully resolved (32–34). Despite the apparent complexity in VEGFR signaling, activation of KDR alone is sufficient to promote all of the major phenotypic responses to VEGF, including endothelial cell proliferation, migration, and survival, and the induction of vascular permeability (35–37).

A variety of methodologies for inhibiting VEGF signal transduction are technically feasible. These include the use of antibodies for ligand sequestration or receptor antagonism, which are currently under clinical investigation (38, 39). An alternative approach is to generate a low molecular weight inhibitor of the KDR tyrosine kinase domain, preferably as an oral therapy, suitable for chronic administration and continual restraint of angiogenesis. We have demonstrated previously that this is possible experimentally with the anilinoquinazoline ZD4190 (40). Subsequent development of ZD4190 revealed that this compound had variable and low oral bioavailability (<5%) in nonrodent species, which was attributed to its modest solubility (41). We now report another heteroaromatic-substituted anilinoquinazoline, ZD6474, which has significantly greater solubility (470-fold more soluble at pH 7.4) and improved oral bioavailability in nonrodent species (>50%), when compared with ZD4190 (41). ZD6474 is currently in Phase I evaluation for the treatment of cancer. Here we describe the ability of ZD6474 to inhibit VEGF signaling, tumor-induced neovascularization, and growth of human xenograft and syngeneic tumor models *in vivo*. The compound achieves greater activity in human tumor models than ZD4190, when examined at equivalent doses of ≥50 mg/kg/day. In addition, the effect on well-established human tumor xenografts was examined, and ZD6474 was found to induce profound regression in PC-3 prostate tumors (0.9–1.4 cm³ pretreatment volume).

MATERIALS AND METHODS

ZD6474 and Recombinant Proteins. ZD6474 [*N*-(4-bromo-2-fluorophenyl)-6-methoxy-7-[(1-methylpiperidin-4-yl)methoxy]quinazolin-4-amine; Fig. 1] was synthesized as described by Hennequin *et al.* (41). Flt-4 and c-kit tyrosine kinases were obtained from ProQuinase GmbH (Freiburg, Germany), and AKT and PDK1 serine-threonine kinases were obtained from Dundee University (Dundee, United Kingdom). All other receptor tyrosine kinases used in isolated enzyme assays were generated as insect cell lysates after cell infection with recombinant baculoviruses containing kinase domains. Human VEGF$_{165}$ and bFGF were similarly prepared using *Spodoptera frugipedera* 21 insect cells and *Escherichia coli* strain BL21(DE3)pLysS respectively, and purified using a heparin-Sepharose column. EGF was obtained from R & D Systems (Abingdon, United Kingdom).

Kinase Inhibition. The ability of ZD6474 to inhibit the kinase activity associated with the VEGFRs KDR, Flt-1, and Flt-4 was determined using a

Fig. 1. Chemical structure of ZD6474.

previously described ELISA (42). Briefly, ZD6474 was incubated with enzyme, 10 mM MnCl₂, and 2 μM ATP in 96-well plates coated with a poly(Glu, Ala, Tyr) 6:3:1 random copolymer substrate (Sigma, Poole, United Kingdom). Phosphorylated tyrosine was then detected by sequential incubation with a mouse IgG anti-phosphotyrosine 4G10 antibody (Upstate Biotechnology Inc., Lake Placid, NY), a horseradish peroxidase-linked sheep antimouse immunoglobulin antibody (Amersham, Little Chalfont, United Kingdom), and 2,2'-azino-bis(3-ethylbenzthiazoline-6-sulfonic acid) (Boehringer, Lewes, United Kingdom). Microcal Origin software (Version 3.78; Microcal Software Inc., Northhampton, MA) was used to interpolate IC₅₀ values by nonlinear regression (4-parameter logistic equation). This methodology was adapted to examine selectivity *versus* tyrosine kinases associated with EGFR, PDGFRβ, Tie-2, FGFR1, c-kit, erbB2, IGF-1R, and FAK. All enzyme assays (tyrosine or serine-threonine) used appropriate ATP concentrations at or just below the respective K_m (0.2–14 μM). Selectivity *versus* serine-threonine kinases (CDK2, AKT, and PDK1) was examined using a relevant scintillation proximity-assay (SPA) in 96-well plates. CDK2 assays contained 10 mM MnCl₂, 4.5 μM ATP, 0.15 μCi of [γ-³³P]ATP/reaction (Amersham Biosciences United Kingdom Ltd., Buckinghamshire, United Kingdom), 50 mM HEPES (pH 7.5), 1 mM DTT, 0.1 mM sodium orthovanadate, 0.1 mM sodium fluoride, 10 mM sodium glycerophosphate, 1 mg/ml BSA fraction V (Sigma-Aldrich, Dorset, United Kingdom), and a retinoblastoma substrate (part of the retinoblastoma gene, 792–928, expressed in a glutathione *S*-transferase expression system; 0.22 μM final concentration). Reactions were allowed to proceed at room temperature for 60 min before quenching for 2 h with 150 μl of a solution containing EDTA (62 mM final concentration), 3 μg of a rabbit immunoglobulin anti-glutathione *S*-transferase antibody (Molecular Probes) and protein A SPA-polyvinyltoluene beads (0.8 mg/reaction; Amersham). Plates were then sealed, centrifuged (1200 × g for 5 min), and counted on a Topcount NXT Microplate scintillation counter (Packard Instrument Co.) for 30 s.

AKT and PDK1 assays were performed with a reaction buffer containing 50 mM Tris-HCl (pH 7.5), 15 mM magnesium acetate, 0.1 mM EGTA, 5 mM DTT, and 0.1 mg/ml BSA fraction V. In the AKT assay, ZD6474 in DMSO [1% (v/v) final assay concentration] was added to a reaction mixture containing buffer, 0.2 μg/ml AKT (delta PH domain previously phosphorylated on S473 by active MAPK-activated protein kinase-2 and T308 by PDK1), 14 μM ATP, 0.1 μCi of [γ-³³P]ATP/reaction, and 6.5 μM of a biotinylated Crosstide substrate [Bachem (United Kingdom) Ltd., St Helens, United Kingdom]. Plates were sealed and incubated at 30°C for 75 min, and the reaction was stopped by the addition of a well-mixed suspension of streptavidin-SPA beads (0.8 mg/reaction, Amersham) and cesium chloride (1 M final assay concentration) in a 50 mM Tris-HCl (pH 7.5) buffer containing 0.05% (w/v) sodium azide. Plates were resealed, incubated at room temperature for 15 min, centrifuged (960 × g for 2 min), transferred to a Topcount, and counted for 30 s (after 15 min for dark adaptation).

In PDK1 assays, ZD6474 was added to an equivalent volume of buffer (10 μl) containing Akt^{Ser473} substrate (3 μg/ml final concentration) and cold ATP (7.5 μM). PDK1 (4 ng in 10 μl of buffer) was then added to each well, and the plates were sealed, agitated, and left at room temperature for 2 h. Next, a mixture (10 μl) of biotinylated Crosstide (5 μM final concentration) and 0.1 μCi of [γ-³³P]ATP/reaction was added, and plates were reagitated and incubated at room temperature for 1 h. Reactions were stopped and counted as described in the AKT assay.

The dual specificity kinase MEK was also examined using a [γ-³³P]ATP-based assay, but with a MAPK substrate and myelin basic protein (Sigma) to capture radioactivity onto filters. The compound was added to a MEK/MAPK premix containing 100 mM EGTA, 1 mg/ml BSA, 1 mM sodium orthovanadate, 14 mM β-mercaptoethanol, and 0.03% polyoxyethylene 23 lauryl ether (Brij-35; Sigma Diagnostics), with 35 μg/ml c-raf-activated MEK and 1.3 μg/ml MAPK. The reaction was started by the addition of ATP and magnesium acetate to a final concentration of 10 μM and 10 mM, respectively. After 1 h at room temperature, [γ-³³P]ATP and myelin basic protein were added to a final concentration of 5.5 μCi and 275 μg/ml, respectively. The reaction was stopped after 10 min at room temperature by the addition of phosphoric acid (12.5% final concentration). The product of the reaction was harvested by paper capture and analyzed by scintillation counting.

Inhibition of Growth Factor-mediated Endothelial Cell Proliferation. HUVEC proliferation in the presence and absence of growth factors was evaluated using [³H]thymidine incorporation (42). Briefly, HUVECs isolated
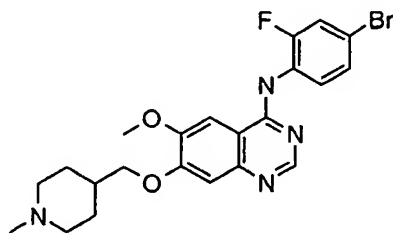
from umbilical cords were plated (at passage 2–8) in 96-well plates (1000 cells/well) and dosed with ZD6474 ± VEGF or EGF (3 ng/ml) or bFGF (0.3 ng/ml). The cultures were incubated for 4 days (37°C; 7.5% CO_2) and then pulsed with 1 μCi/well [^{3}H]thymidine (Amersham) and reincubated for 4 h. Cells were harvested and assayed for the incorporation of tritium using a beta counter. IC_{50} data were interpolated as described above.

Inhibition of an Acute VEGF-induced Hypotension in Rat. Methodology to enable blood pressure measurement in anesthetized rats was as described previously (43). Briefly, anesthesia was induced in male Alderley Park rats (Wistar derived, 230–280 g in weight) using α-chloralose (Sigma, Dorset, United Kingdom) by the i.v. route and then maintained with thiopentone (Intraval; May & Baker) via the i.p. route. Once surgical anesthesia was established, the carotid artery was cannulated to enable blood pressure recording using a pressure transducer (Bell and Howell Ltd., Basingstoke, United Kingdom) and a Lectromed MT8P amplifier (Lectromed United Kingdom Ltd., Letchworth, United Kingdom). The jugular vein was cannulated to allow growth factor administration. Body temperature was maintained with a thermostatically controlled heated blanket coupled to a rectal thermometer (Harvard Apparatus Ltd., Edenbridge, United Kingdom). Human $VEGF_{165}$ (32 μg/kg) or bFGF (40 μg/kg) was administered as a bolus injection [0.1 ml/250 g body weight in 0.85% (w/v) sodium chloride], and a maximal blood pressure drop was recorded within 2 min (typically 26–30 mm Hg). These changes were sustainable for more than 20 min in control experiments. ZD6474 (2.5 mg/kg) or vehicle alone [25% (w/v) hydroxypropyl-β-cyclodextrin in Sorensons phosphate buffer (pH 5.5)] was administered i.v., and blood pressure was recorded 5 min later to determine the effect on growth factor-induced hypotension.

Epiphyseal Growth Plate Hypertrophy in Rat. For all additional *in vivo* work, ZD6474 was suspended in a 1% (v/v) solution of polyoxyethylene (20) sorbitan mono-oleate in deionized water and administered by oral gavage. Young female Alderley Park rats (Wistar derived, 150 g in weight, 4–8 weeks of age) were dosed daily for 14 days with ZD6474 (at 0.25 ml/100 g body weight) or vehicle. Morphometric image analysis of femoro-tibial sections was performed as described previously (40). Growth plate areas from the femur and tibia in each joint were combined for an analysis of the effect of compound treatment.

Tumor Cell Lines. Seven human tumor cell lines were used [PC-3 (prostate adenocarcinoma), Calu-6 and A549 (lung carcinoma), MDA-MB-231 (mammary gland adenocarcinoma), SKOV-3 (ovarian adenocarcinoma), A431 (vulval carcinoma), and SW620 (colorectal carcinoma)], each of which was obtained from the American Type Culture Collection (Manassas, VA). Two murine tumor cell lines, Lewis Lung and B16-F10, were also obtained from the American Type Culture Collection, and a syngeneic subclone of B16-F10 [B16-F10(AP3)] was generated by three rounds of serial *in vivo* passage (*i.e.,* i.v. inoculation of 1 × 10^5 B16-F10 cells in AP C57/BL6 mice and recovery of tumor cells from a tumor deposit in the lungs). Each cell line was maintained as an exponentially growing monolayer, and all cell culture reagents, where not specified, were obtained from Life Technologies, Inc. (Paisley, United Kingdom). Culture conditions for PC-3, Calu-6, MDA-MB-231, and SKOV-3 cells were as described previously (40). A431, A549, Lewis Lung, and B16-F10(AP3) cells were cultured in DMEM with 2 mM L-glutamine (Sigma, Poole, United Kingdom) and 5% (A431) or 10% FCS (Labtech International, Ringmer, United Kingdom). Media for A431 were supplemented with 1% nonessential amino acids (Life Technologies, Inc.). This supplement was also used in media for B16-F10(AP3) cells, with the further addition of 1% MEM vitamins (Life Technologies, Inc.) and 1% pyruvate (1 mM final concentration; Sigma). SW620 cells were grown in L15 (non-CO_2-equilibrated) media (Life Technologies, Inc.) containing 10% FCS and 2 mM glutamine. All cell lines were maintained at 37°C with 7.5% CO_2, except for SW620 cells, for which CO_2 was excluded. Cell lines were periodically screened for the presence of *Mycoplasma* in culture and analyzed for 15 types of virus in a mouse antibody production test (Syngenta, Alderley Park, United Kingdom) before routine use *in vivo*.

Tumor Cell Cytotoxicity Assay. Tumor cells were plated in their respective media at predetermined densities that were known to enable logarithmic cell growth during the period of assay (PC-3, 500 cells/well; all others, 1000 cells/well). Plates were incubated for 24 h (37°C with CO_2 as described) before the addition of ZD6474 (0.1–100 μM) or vehicle (0.1% DMSO in medium). Plates were reincubated for an additional 72 h before assessing cell proliferation by [^{3}H]thymidine incorporation as described in HUVEC experiments.

In Vivo Tumor Models. Tumor implantation procedures were performed on mice of at least 8 weeks of age. All mice were bred and maintained at Alderley Park, provided with sterilized food and water *ad libitum*, and housed in a barrier facility with 12-h light/dark cycles. Human tumor xenografts were grown in female athymic (*nu/nu* genotype) Swiss mice housed in negative pressure isolators (PFI Systems Ltd., Oxford, United Kingdom), and syngeneic tumors were grown in C57/BL6 mice.

Intradermal Tumor Angiogenesis. To visualize the induction of angiogenesis by a tumor *in vivo*, an intradermal tumor model was used. In this model, neovasculature, observed predominantly at the tumor periphery, can be quantified by vessel counting (44, 45). Male nude mice were anesthetized (inhalant 4% Halothane-vet; Merial Animal Health Ltd., Essex, United Kingdom), and 10^7 A549 human lung tumor cells in 50 μl of PBS (Dulbecco's pH 7.4, without calcium chloride and magnesium chloride; Sigma) were implanted intradermally at two sites in the abdominal region. Two additional injections of PBS (50 μl) were performed on each mouse as a control. All implant sites were marked with indelible ink to aid identification at the end of the experiment. Mice were allowed to recover fully from anesthesia before being dosed p.o. with ZD6474 (50 or 100 mg/kg/day) or vehicle (4 mice/group). Daily dosing was continued for a total period of 5 days. Each mouse was humanely culled 24 h after the last dose of ZD6474 or vehicle, and a section of the abdominal wall skin encompassing all implant sites was removed and spread onto filter paper. Sections were examined by light microscopy (×10 magnification), and the total number of blood vessels (major vessels and branching points) was determined within a 1-cm^2 area around each implant site. Vessel counts from implants of PBS were consistent irrespective of treatment; the mean value (27 ± 1.2; mean ± SE) was therefore subtracted from control and ZD6474-treated vessel counts to give a more accurate indication of tumor-induced blood vessel formation and to ascertain the effect of treatment.

s.c. Tumor Models. Protocols for establishing s.c. PC-3, Calu-6, SKOV-3, and MDA-MB-231 tumors were as described previously (40). SW620 and A549 tumors were established by s.c. injection of 1 × 10^6 and 5 × 10^6 cells, respectively, in 100 μl of serum-free media containing 50% Matrigel (Fred Baker, Liverpool, United Kingdom), into the hind flank of mice. A431 tumors were also initially established in the same way but were used (10–14 days after inoculation) to generate cubic tumor fragments of 0.5–1 mm^3 in diameter, which were implanted for therapy experiments. Mice were randomized into groups of 10 before treatment at a point when tumors reached a volume of 0.15–0.47 cm^3. Mice then received (p.o.) either ZD6474 (12.5–100 mg/kg/day) or vehicle, administered once daily at 0.1 ml/10 g body weight. Subsequent experiments also examined treatment of much larger tumors (up to 1.4 cm^3 in volume). For studies examining rodent tumors, B16-F10(AP3) cells (1 × 10^5 cells in 100 μl) or a suspension of disaggregated Lewis Lung tumor cells (recovered from established tumors; 50-μl volume), in PBS without calcium chloride or magnesium chloride (Life Technologies, Inc.), was implanted s.c. Because these syngeneic models have aggressive growth characteristics, ZD6474 (25–100 mg/kg/day) or vehicle was dosed p.o. from the day of tumor implantation. Tumor volumes were assessed at least twice weekly by bilateral Vernier caliper measurement and calculated (taking length to be the longest diameter across the tumor and width to be the corresponding perpendicular diameter) using the formula (length × width) × $\sqrt{}$(length × width) × (π/6). Growth inhibition from the start of treatment was assessed by comparison of the differences in tumor volume between control and treated groups. Because the variance in mean tumor volume data increases proportionally with volume (and is therefore disproportionate between groups), data were log-transformed to remove any size dependency before statistical evaluation. Statistical significance was evaluated using a one-tailed two-sample *t* test.

Histological Analysis of Calu-6 Tumors. Calu-6 tumors from a s.c. tumor xenograft experiment, treated with vehicle or ZD6474 (25–100 mg/kg/day) once daily for 24 days, were collected for histological analysis. Half of each tumor was fixed in 10% buffered formalin, and the other half was fixed in zinc fixative (BD PharMingen, Oxford, United Kingdom) for 24 h, before being processed to paraffin wax. Sections (3 μm) were produced by standard histological techniques. To visualize endothelial cells, CD31 was detected in zinc-fixed tissue using an avidin-biotin method. Briefly, endogenous peroxidase was blocked with 3% hydrogen peroxide (30 min), and nonspecific background staining was blocked with normal rabbit serum (1:20 dilution; Dako, Cambridgeshire, United Kingdom). Sections were incubated (1 h) with a monoclonal rat antimouse CD31 primary antibody (1:500 dilution; BD

PharMingen), followed by a 30-min incubation with a mouse adsorbed bioti-nylated rabbit antirat immunoglobulin (1:200 dilution; Dako) and a further 30-min incubation with a StreptABComplex conjugated with horseradish peroxidase (Dako). Visualization was by a diaminobenzidine (Biogenex, Berk-shire, United Kingdom) chromogen procedure. Sections were analyzed using a Zeiss KS400 (Version 3.0) image analyzer (Imaging Associates Ltd., Thame, United Kingdom), which counted up to six randomly selected fields of view at ×1.6 objective lens magnification encompassing only viable tumor tissue (i.e., excluding areas of necrosis) to enable the determination of CD31 positive area/5000 μm^2 viable tumor. To visualize necrosis, formalin-fixed, paraffin wax-embedded tissue sections were stained with H&E, and the relative area of necrotic tissue:total tumor area was determined visually, using interactive textual region detection morphometric image analysis of the whole tumor section. To visualize apoptosis, the Roche in situ cell death detection kit (Roche, Lewes, United Kingdom) was used, which incorporates the TUNEL technique. In brief, formalin-fixed, paraffin wax-embedded tissue sections were treated with proteinase K (2 min; Dako) and blocked for endogenous peroxidase using 3% hydrogen peroxide. Sections were then incubated for 1 h at 37°C in TUNEL reaction mixture, followed by a 30-min incubation with converter-Pod (peroxidase). Visualization was by a diaminobenzidine (Bio-genex) chromogen procedure.

RESULTS

Inhibition of KDR Tyrosine Kinase and Selectivity. In ELISAs with recombinant enzymes, ZD6474 is a potent inhibitor of KDR tyrosine kinase activity (IC$_{50}$ = 40 nM) and a submicromolar inhibitor of EGFR tyrosine kinase (IC$_{50}$ = 500 nM; Table 1). The compound has activity versus the kinase activity of the VEGF-C and -D receptor Flt-4 (IC$_{50}$ = 108 nM) but has significantly less activity versus Flt-1 (IC$_{50}$ = 1600 nM). Excellent selectivity for KDR was demonstrated versus additional tyrosine kinases (PDGFRβ, Tie-2, FGFR1, c-Kit, erbB2, IGF-IR, and FAK), serine-threonine kinases (CDK2, AKT, and PDK1), and the dual specificity kinase MEK (Table 1).

Inhibition of VEGF-induced Mitogenesis in Endothelial Cells. The activity versus isolated KDR in enzyme assays translated into potent inhibition of VEGF-stimulated HUVEC proliferation in vitro, as judged by [^{3}H]thymidine incorporation (IC$_{50}$ = 60 nM; Fig. 2). No effect was observed on basal endothelial cell growth (2% serum) with a >50-fold concentration of ZD6474. The ZD6474 selectivity profile observed in the recombinant enzyme assay (i.e., inhibition of VEGF > EGF > bFGF) was also evident in this growth factor-

Table 1 *ZD6474 kinase selectivity*

Kinase	IC$_{50}$ (μM)[a]	Fold selectivity vs. KDR[b]
KDR	0.04 ± 0.01	
Flt-4	0.11 ± 0.02	2.7
Flt-1	1.6 ± 0.4	40
EGFR	0.5 ± 0.1	12.5
PDGFRβ	1.1 ± 0.3	27.5
Tie-2	2.5 ± 1.2	62.5
FGFR1	3.6 ± 0.9	90
MEK	>10	>250
CDK2	>10	>250
c-kit	>20	>500
erbB2	>20	>500
FAK	>20	>500
PDK1	>20	>500
AKT	>100	>2500
IGF-IR	>200	>5000

[a] The ability of ZD6474 to inhibit recombinant tyrosine kinase activity was examined using 96-well ELISAs, whereas activity against serine-threonine kinases and the dual specificity kinase MEK was examined using scintillation proximity-based assays (refer to "Materials and Methods" section for details). ATP concentrations were at or just below the respective K$_m$ (0.2–14 μM). Data represent the mean ± SE of at least three separate determinations. IC$_{50}$ values quoted as "greater than" denote the inability to reach an IC$_{50}$ value with the highest concentration tested.

[b] Ratio for the IC$_{50}$ obtained with a given kinase compared to that achieved versus KDR.
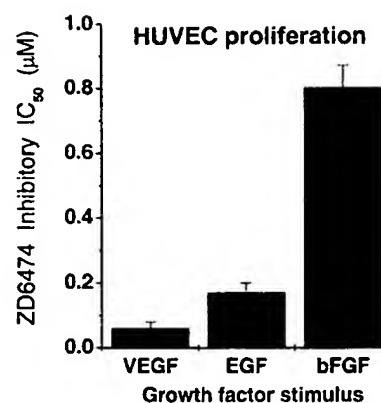

Fig. 2. Inhibition of VEGF-stimulated endothelial cell proliferation. The effect of ZD6474 on growth factor-stimulated (3 ng/ml VEGF or EGF or 0.3 ng/ml bFGF) HUVEC growth was examined using [^{3}H]thymidine incorporation to assess proliferation. Data represent the mean ± SE of five to six independent experiments. Basal HUVEC growth was not inhibited at a ZD6474 concentration of 3 μM.

stimulated HUVEC proliferation assay, with IC$_{50}$ values of 170 and 800 nM for EGF- and bFGF-stimulated cell growth, respectively.

Effects on Tumor Cells in Vitro. The ability of ZD6474 to inhibit tumor cell growth directly was examined in vitro. IC$_{50}$ values (mean ± SE; n = 3 separate determinations) for the inhibition of tumor cell growth by ZD6474 ranged from 2.7 ± 0.5 μM (A549) to 13.5 ± 1.5 μM (Calu-6). These concentrations are between 45- and 225-fold greater than those required to inhibit VEGF-stimulated HU-VEC proliferation.

Inhibition of VEGF Signaling Responses in Vivo. For confirmation of inhibition of VEGF signaling and angiogenesis in vivo, two pharmacodynamic end points were examined in rat. Several growth factors (including VEGF) have been shown to induce a profound hypotension in anesthetized rats when administered as a large bolus dose. This effect is attributed to a specific signaling response through the growth factor's cognate receptor to which tachyphylaxis can be demonstrated (46). ZD6474 (2.5 mg/kg, i.v.), reversed a VEGF-induced hypotension (by 63%; P < 0.001) but did not significantly affect a bFGF-induced hypotension (Fig. 3a). These data support inhibition of VEGF signaling in vivo by ZD6474, and the selectivity observed is consistent with that observed in tyrosine kinase and HUVEC proliferation assays. The effect of ZD6474 on growth plate morphology was also examined because angiogenesis is a prerequisite for ossification during long bone extension, and vascular invasion of the growth plate is dependent on VEGF secretion from hypertrophic chondrocytes (47). ZD6474 produced a dose-dependent hypertrophy of the femoro-tibial growth plates of young growing rats when administered once daily (p.o.) for 14 days (Fig. 3b). Doses of 50 and 100 mg/kg/day ZD6474 increased the combined growth plate area by 57% and 75%, respectively (P < 0.001, one-tailed two-sample t test).

Intradermal Tumor Angiogenesis. A549 tumor cells implanted intradermally (2 implant sites/mouse; 4 mice/group) were found to induce significant angiogenesis within a period of 5 days, i.e., 152 ± 6.5 vessels compared with a background count of 27 ± 1.2 vessels in vehicle implants (mean ± SE). Oral administration of 50 or 100 mg/kg/day ZD6474 for 5 days inhibited the tumor-induced blood vessel formation by 63% and 79%, respectively (P < 0.001; Fig. 4).

Inhibition of Tumor Growth. Chronic once-daily oral administration of ZD6474 produced a dose-dependent inhibition of tumor growth in all models examined (Table 2). Statistical significance was evident in each tumor xenograft model with administration of 25 mg/kg/day (P < 0.05 in SKOV-3 and P < 0.001 in all others). Of the seven human tumor xenografts studied, five were also significantly

(a) Inhibition of VEGF-Induced Hypotension

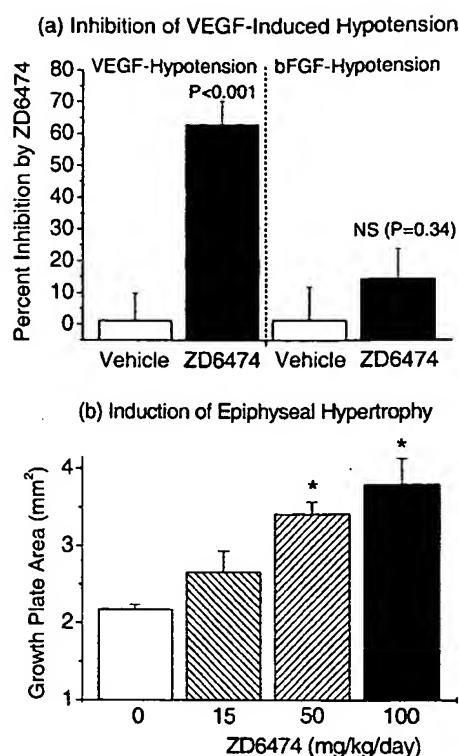## (b) Induction of Epiphyseal Hypertrophy

Fig. 3. Inhibition of VEGF signaling responses *in vivo*. *a*, ZD6474 inhibits an acute VEGF-induced hypotension. We have previously described the use of the anesthetized rat to show the acute hypotensive effects of large doses of VEGF or bFGF and tachyphylaxis. VEGF (8 µg/ml) or bFGF (20 µg/ml) was administered as a bolus i.v. injection, and a drop in blood pressure was induced (26–30 mm Hg). ZD6474 (2.5 mg/kg, i.v.) reversed a VEGF-induced hypotension by 63% (*P* < 0.001) but did not significantly affect that induced by bFGF (4–6 rats/group, mean + SE). Although there appears to be a marginal effect on bFGF-induced hypotension, this can be attributed to a single outlier in the data set. *b*, ZD6474 induces epiphyseal growth plate hypertrophy. Young rats were treated once daily for 14 days with vehicle or ZD6474 (15–100 mg/kg/day, p.o.). Morphometric image analysis was performed on the femoral and tibial epiphyseal growth plates. ZD6474 produced a dose-dependent increase in the combined epiphyseal growth plate area (5–6 rats/group, *, *P* < 0.001 by one-tailed *t* test).

growth-inhibited by administration of 12.5 mg/kg/day ZD6474 (*P* < 0.01). Full growth inhibition profiles are shown for four of the xenograft models (Fig. 5). ZD6474 treatment was well tolerated, with only small effects on body weight (particularly at ZD6474 doses of ≤50 mg/kg/day) and no adverse effects on clinical condition (even at 100 mg/kg/day for 5 weeks). When body weights of mice from all seven xenograft experiments were analyzed, treatment with 12.5, 25, 50, or 100 mg/kg/day ZD6474 for 3 weeks induced mean body weight losses of 0.3%, 2.2%, 3.8%, and 7.7%, respectively, when compared with pretreatment values, whereas vehicle-treated controls gained 1.8% body weight during this period. Similar effects on body weight were observed when ZD6474 was administered for a longer duration; in the PC-3 xenograft experiment, treatment with 12.5, 25, 50, or 100 mg/kg/day ZD6474 for a total of 5 weeks induced mean body weight losses of 1.4%, 1.0%, 2.6%, and 10%, respectively, whereas vehicle-treated controls remained at their starting (pretreatment) mean body weight. The activity of ZD4190, a predecessor of ZD6474, had been examined previously in Calu-6, MDA-MB-231, PC-3, and SKOV-3 tumors (40). ZD6474 consistently produced a greater inhibition of tumor growth than ZD4190 when compared at doses of 50 and 100 mg/kg/day in these models (Fig. 6), although this just failed to reach statistical significance at 50 mg/kg/day in PC-3 (*P* = 0.07). Whereas superior inhibition of tumor growth was not obtained with 100 mg/kg/day ZD6474 in SKOV-3, this was to be expected, given that

ZD4190 inhibited the growth of this tumor completely (*i.e.*, by 95 ± 6%) at this dose (Fig. 6). The effect of ZD6474 treatment on rapidly growing syngeneic tumors in immunocompetent mice was also examined because the tumor:host signaling responses may be reproduced more accurately in these models. ZD6474 also inhibited the growth of these tumors (Fig. 7), with highly significant activity evident at 25 mg/kg/day (Table 2).

Histological Analysis of Calu-6 Tumors. Treatment of Calu-6 tumors with 50 or 100 mg/kg/day ZD6474 (once daily, p.o.) for 24 days reduced CD31 (endothelial cell) staining in viable tumor tissue by >70% when compared with vehicle-treated controls (Fig. 8, *a* and *b*; *n* = 5 mice/group). These treatments were also found to increase the percentage of necrosis within Calu-6 tumors (by 2.7- and 3.2-fold with 50 and 100 mg/kg/day, respectively; Fig. 8*c*). Statistically significant effects on CD31 staining or necrosis were not observed in Calu-6 tumors from mice treated with 25 mg/kg/day ZD6474, despite observing significant tumor growth inhibition. An examination of tumor cell apoptosis in nonnecrotic areas of tumor (using TUNEL) did not reveal differences in the extent or pattern of staining between vehicle-treated controls and any ZD6474-treated group (25–100 mg/kg/day; data not shown).

Effects on Well-established Human Tumor Xenografts. The effect of ZD6474 treatment on much larger tumor xenografts (0.65–1.4 cm³ volume), which may have more established vasculature, was also examined. Treatment of Calu-6 lung tumors of either 0.3 or 0.9 cm³ mean volume at the start of ZD6474 treatment indicated that a comparable inhibition of tumor growth could be obtained (Fig. 9*a*). In contrast, ZD6474 induced regression in established PC-3 prostate tumors of varying sizes (Fig. 9*b*), with the most dramatic effects being produced in the largest tumors (1.4 cm³ tumors regressing to <0.2 cm³ after 3 weeks of treatment).

DISCUSSION

There is a significant unmet need for cytostatic (*i.e.*, noncytotoxic) therapies that can stabilize or slow the progression of solid tumor disease, particularly in non-hormone-dependent cancers. One approach may be to inhibit VEGF signaling, given its central role in angiogenesis, which is thought to be necessary for all macroscopic solid tumor growth. Extrapolation from anti-hormonal treatments suggests that chronic dosing is likely to be required, and therefore an oral therapy may be preferable for greater patient convenience. We have previously reported identification of a p.o.-active VEGFR TKI, ZD4190, which demonstrated promising activity in preclinical tumor models (40). Improvement of both the physicochemical and pharmacokinetic properties of ZD4190 led to the discovery of several new agents, including the anilinoquinazoline ZD6474, which was selected for clinical development.

In recombinant enzyme assays, ZD6474 is a potent inhibitor of KDR activity (VEGFR2; IC_{50} = 40 nM), with additional activity *versus* the tyrosine kinase of the VEGF-C and -D receptor Flt-4 (VEGFR3; IC_{50} = 110 nM) and comparatively less activity *versus* that of Flt-1 (VEGFR1; IC50 = 1600 nM).

Because KDR has the predominant role in mediating VEGF signal transduction in endothelial cells (35–37), this profile is compatible with the aim of developing a VEGF signaling inhibitor. Although the quantitative relationship between enzyme and cell data was examined for KDR (*i.e.*, by comparison with inhibition of VEGF-induced HUVEC proliferation), this relationship was not determined for Flt-1 and Flt-4. Flt-1 has the highest affinity for VEGF but yields a comparatively weak autophosphorylative response and does not induce mitogenesis in endothelial cells (31, 48, 49). This receptor may act as a negative regulator of angiogenesis by sequestering VEGF (50). Re-
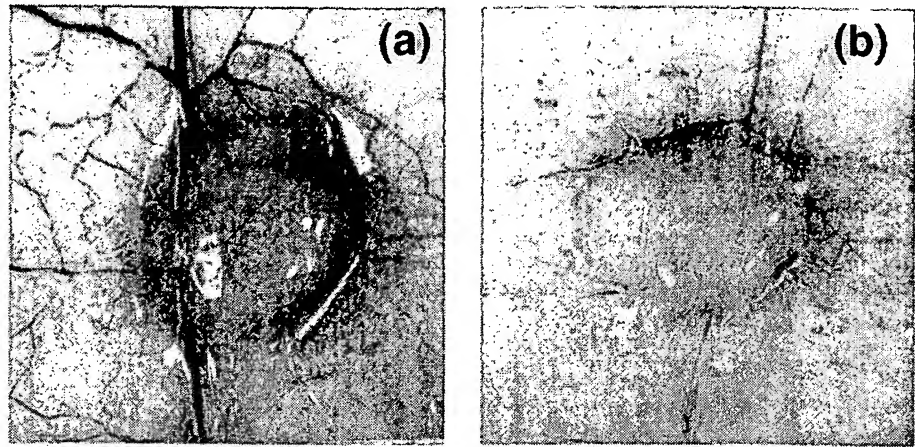
Fig. 4. Effect of ZD6474 on tumor-induced angiogenesis. To visualize the induction of angiogenesis by a tumor *in vivo*, A549 tumor cells were implanted intradermally, and new blood vessel formation was assessed 5 days later by light microscopy. The effect of administering (a) vehicle or (b) 100 mg/kg/day ZD6474 for the duration of assay (once daily, p.o.) is shown in representative images (×1 objective magnification). The total number of blood vessels (major vessels and branching points) was determined within a precise 1-cm² area around each implant site (2/mouse, 4 mice/group; refer to "Materials and Methods" for full details). Mean vessel count data (c) indicate that ZD6474 administration inhibited tumor-induced angiogenesis significantly (by 63% and 79% with 50 and 100 mg/kg/day ZD6474, respectively). *, $P < 0.001$ by one-tailed t test.
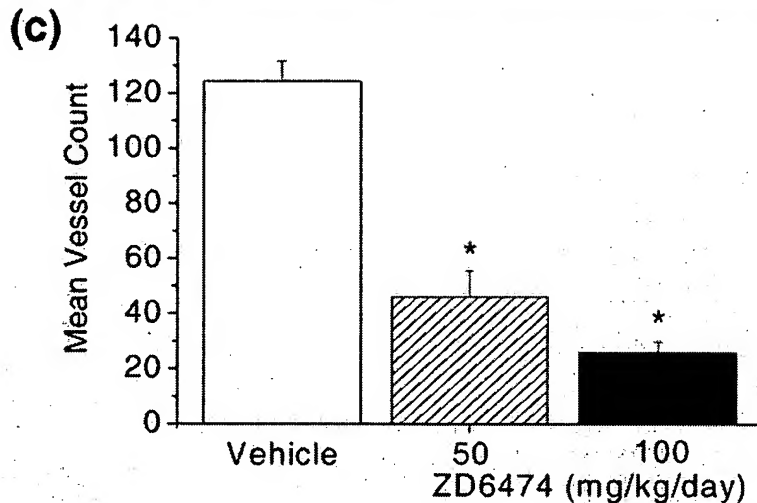
cent data suggest that Flt-1 signaling may be of consequence in pathological angiogenesis (51) but potentially only by virtue of its ability to transactivate KDR. Flt-4 was initially thought to be restricted to lymphatic endothelium (28) and therefore of less relevance to tumor angiogenesis. However, recent data suggest that Flt-4 can be elevated on tumor blood vessels during neovascularization (52, 53) and that tumor VEGF-C expression can correlate with lymphatic invasion, increased metastasis, and a worse clinical prognosis (54, 55). Hence, if the inhibition of Flt-4 tyrosine kinase by ZD6474 translates into potent inhibition of Flt-4 signaling in cells, then this activity could potentially also impart a therapeutic benefit.

It is highly likely that ZD6474 adopts a kinase binding conformation, in which the adenine binding site of the kinase is occupied by the quinazoline ring, and the aniline of the molecule fits into a hydrophobic pocket that is structurally distinct between different kinases. By exploiting the nonconserved features of the KDR kinase domain, ZD6474 can achieve selectivity *versus* a range of tyrosine and serine-threonine kinases, including those of structurally related receptors (*e.g.*, Flt-1, PDGFRβ, and c-kit). However, although apparent selectivity for inhibition of KDR tyrosine kinase is evident *versus* many other kinases, ZD6474 was also found to elicit submicromolar activity *versus* that associated with EGFR. The activity of ZD6474 *versus* KDR tyrosine kinase translated into potent inhibition of VEGF signaling in human primary endothelial cells, with prevention of VEGF-induced proliferation (IC50 = 60 nM). Notably, the inhibition of VEGF signaling by ZD6474 occurs at concentrations well below

those that show significant direct effects on the normal growth of endothelial (>3 μM) or tumor cells (2.7–13.5 μM).

Large i.v. doses of VEGF ($\geq$10 μg/kg) have been shown to induce an acute hypotensive effect in anesthetized rats. This effect is thought to depend on VEGF receptor signaling because VEGF induces a rapid desensitization to itself (tachyphylaxis) but does not produce desensitization to hypotension induced by other growth factors, such as bFGF (43). Both VEGF- and bFGF-induced hypotension are dependent on production of nitric oxide because either response can be abolished with the nitric oxide synthase inhibitor N-nitro-L-arginine methyl ester (56, 57). The observation that ZD6474 was able to reverse a VEGF-induced hypotension in rat but did not significantly affect that induced by bFGF is concordant with selective inhibition of VEGF signaling *in vivo*. ZD6474 also produced a dose-dependent hypertrophy of the femoro-tibial growth plates of young growing rats when administered p.o. for 14 days, which is to be expected, given the role of VEGF in bone morphogenesis (58). VEGF expression by hypertrophic chondrocytes is thought to drive the angiogenesis needed for endochondral ossification. Similar effects on long bone growth plates have been reported previously with a VEGF antibody (59) and a soluble VEGFR construct (47) that selectively sequester VEGF. Increased hypertrophic chondrocyte numbers have also been induced in the long bones of mice after Cre-lox-mediated VEGF deletion in cartilage using the collagen 2a1 promoter (60). Collectively, these data in rat indicate that ZD6474 inhibits VEGF signaling and angiogenesis *in vivo*.

Table 2 *Chronic oral once-daily administration of ZD6474 inhibits tumor growth*

Human tumor xenografts were established in the hind flank of Swiss athymic mice (8–12 weeks of age). Mice were randomized (10 mice/group) when tumors reached a volume of 0.15–0.47 cm^3 and then treated with oral daily doses of ZD6474 (12.5–100 mg/kg/day) or vehicle [a 1% (v/v) solution of polyoxyethylene (20) sorbitan mono-oleate in deionized water]. Syngeneic tumors were implanted s.c. in the hind flank of C57/BL6 mice (10 mice/group) and treated with ZD6474 (25–100 mg/kg/day, p.o.) or vehicle from the day of tumor implantation. Percentage tumour growth inhibition was calculated as the difference between the change in control and ZD6474-treated tumor volumes over the period of treatment. Statistical significance was examined on log-transformed data using a one-tailed t test (NS, not significant, $P > 0.05$).

Tumor model	Tumor origin	ZD6474 dose (p.o.) mg/kg/day	No. of doses	% Inhibition of tumor volume	P
Calu-6	Human lung	100	28	92	<0.001
		50		78	<0.001
		25		56	<0.001
		12.5		57	<0.001
PC-3	Human prostate	100	35	>100	<0.001
		50		95	<0.001
		25		68	<0.001
		12.5		29	NS (0.06)
MDA-MB-231	Human breast	100	25	99	<0.001
		50		83	<0.001
		25		63	<0.001
		12.5		73	<0.001
SKOV-3	Human ovary	100	28	100	<0.001
		50		98	<0.001
		25		50	<0.05
		12.5		31	NS (0.3)
SW620	Human colon	100	22	91	<0.001
		50		77	<0.001
		25		46	<0.001
		12.5		26	<0.01
A549	Human lung	100	25	>100	<0.001
		50		>100	<0.001
		25		89	<0.001
		12.5		64	<0.001
A431	Human vulva	100	21	>100	<0.001
		50		>100	<0.001
		25		80	<0.001
		12.5		48	<0.01
B16-F10(AP3)	Murine melanoma	100	17	92	<0.001
		50		77	<0.001
		25		56	<0.01
Lewis Lung	Murine lung	100	14	79	<0.001
		50		70	<0.001
		25		61	<0.001

Chronic once-daily oral administration of ZD6474 (12.5–100 mg/kg/day) produced a dose-dependent inhibition of tumor growth in a panel of human tumor xenograft models, despite their varied histological origin (breast, lung, prostate, colon, ovary, and vulva) and different growth rates. This was also evident in syngeneic tumor models (B16-F10 and Lewis Lung) in immunocompetent animals. In all cases, the percentage inhibition of tumor growth progressively increased as the duration of dosing was extended, which is indicative of a sustained antitumor effect. The broad spectrum activity observed with ZD6474 in tumor models is consistent with inhibition of VEGF signaling and an indirect (*i.e.*, antiangiogenic) antitumor effect rather than direct antiproliferative effects on the tumor cell. Pharmacokinetic modeling (data not shown) suggests that the steady-state free levels of ZD6474 that are capable of producing a highly significant ($P < 0.001$) antitumor effect *in vivo* can be as much as 100-fold less than the free levels required to produce a direct inhibition (IC$_{50}$) of tumor cell proliferation *in vitro*. The profile observed contrasts with that of tumor cell-directed therapies, which would not be expected to retain comparable activity against all tumor models examined. Histological analysis of Calu-6 tumor xenografts also indicated that ZD6474 doses of ≥50 mg/kg, administered for 24 days, reduced CD31 staining in viable tumor tissue and increased the proportion of necrosis within the tumor. However, the proportion of tumor cell apoptosis in areas of viable tumor did not appear to be affected. These data are compatible with inhibition of VEGF signaling because a significant reduction in tumor neovascularization and VEGF-induced vascular permeability could be expected to result in greater tumor ischemia and the induction of tumor cell necrosis.

ZD6474 gave a better antitumor effect than was reported previously with its predecessor ZD4190 (40), when compared at doses of 50 and 100 mg/kg/day (p.o.). The greater effect of ZD6474 is not related to its additional submicromolar activity *versus* EGFR tyrosine kinase because ZD4190 also had activity *versus* this enzyme and proved comparatively more potent in an EGF-stimulated HUVEC proliferation assay (IC$_{50}$ = 50 nM; Ref. 41). The increase in efficacy is most likely attributed to a gain in free drug levels in mouse (4.1% *versus* 2.5%) combined with a pharmacokinetic profile that gives extended plasma exposure until 24 h after administration of a single dose (in rat, the plasma half-life of ZD6474 has been shown to be approximately 12-fold greater than that of ZD4190; Ref. 41). We have previously observed in a series of anilinoquinazolines that extended plasma exposure for the duration of the dosing interval (i.e., for 24 h with once-daily dosing) is required for maximum therapeutic effect in tumor xenograft models (40).

In addition to its anti-VEGF pharmacology, ZD6474 can also inhibit EGFR signaling in cells (IC$_{50}$ for inhibition of EGF-stimulated HUVEC proliferation = 170 nM). EGFR overexpression by tumor cells has been found to correlate with poor prognosis in a range of malignancies (*e.g.*, lung, colorectal, ovarian, breast, head and neck, bladder, ovarian, renal, and gastric cancers; Refs. 61 and 62). This receptor can be activated by a number of structurally related ligands (*e.g.*, EGF and transforming growth factor α), which can be produced
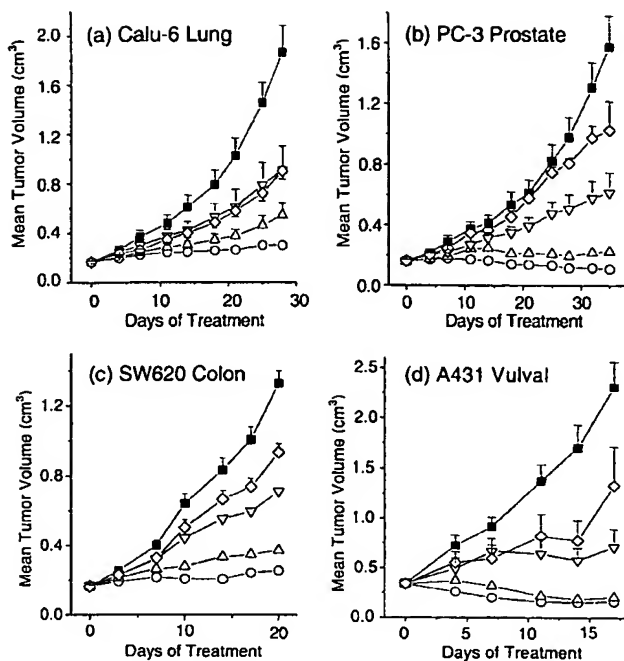
Fig. 5. Effect of ZD6474 (◇, 12.5 mg/kg/day; ▽, 25 mg/kg/day; △, 50 mg/kg/day; ○, 100 mg/kg/day) or vehicle (■) on the growth of selected human tumor xenografts (*a*, Calu-6; *b*, PC-3; *c*, SW620; *d*, A431). Xenografts were established s.c. in athymic mice and allowed to reach a volume of 0.16-0.34 cm³ before treatment. Once-daily oral administration of ZD6474 or vehicle was then started and continued for the duration of the experiment. Data points represent a mean from 10 mice, with SEs shown in one direction.

ing migration, antiapoptosis, and angiogenesis (63–65). Inhibition of EGFR tyrosine kinase is therefore a promising therapeutic strategy in its own right, with antibody [*e.g.*, C225 (66)] and small molecule approaches [*e.g.*, ZD1839 Iressa (67)] currently in late-stage clinical development for the treatment of colorectal cancer and non-small cell lung cancer, respectively. It is possible that EGFR inhibition by ZD6474, particularly at higher doses, may afford additional antitumor activity in tumors that are dependent on EGFR-driven proliferation. From the panel of tumor xenografts examined, A431 and A549 are known to have a specific EGFR signaling dependency (68), and it is interesting to note that when ZD6474 was administered at 50 mg/kg/day, there was evidence of some tumor regression in these two particular models. It is anticipated that the significant inhibition of A549-induced angiogenesis observed in the intradermal tumor angiogenesis model is predominantly a consequence of inhibition of VEGF signaling because this tumor xenograft secretes relatively high levels of VEGF, and similar data have been produced with selective KDR TKIs (data not shown). Nonetheless, it is still feasible that inhibition of EGFR signaling could also contribute to an antiangiogenic effect in an EGFR-dependent tumor, from inhibition of direct EGF-induced angiogenesis and/or EGF-induced VEGF expression by tumor cells (65, 69). The advantages of targeting both EGFR and VEGFR pathways simultaneously have been recently been outlined in a study examining coadministration of antibodies to both KDR and EGFR (70). However, whereas there are potential therapeutic benefits to also inhibiting EGFR tyrosine kinase, this activity is not a prerequisite for obtaining an antitumor effect with ZD6474. Selective EGFR TKIs do
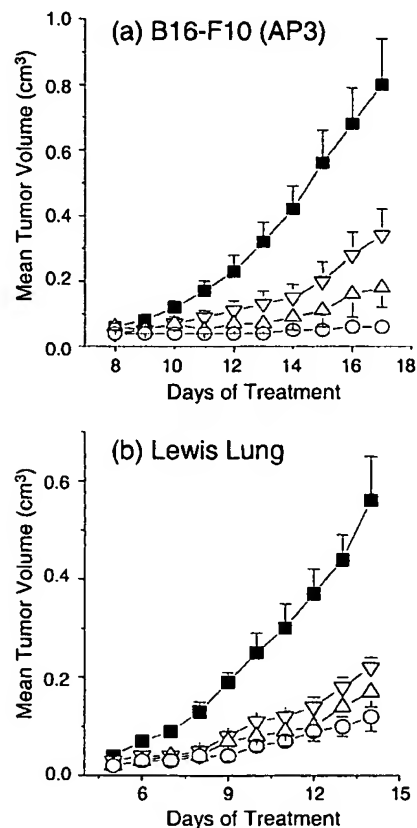

Fig. 6. ZD6474 (■) *versus* ZD4190 (□): comparative activity in (*a*) Calu-6, (*b*) MDA-MB-231, (*c*) PC-3, and (*d*) SKOV-3 human tumor xenografts. Tumor growth inhibition data from previous experiments with ZD4190 (40) were compared with that obtained using ZD6474 at equivalent doses of 50 and 100 mg/kg and after 21 days of treatment. Statistical significance was examined using a one-tailed two-sample *t* test.

in large amounts by epithelially derived tumor cells and induce autocrine-stimulated tumor cell proliferation (61). EGFR signaling has been further implicated in the induction of other tumor and host cell phenotypes that contribute to driving tumor progression, includ-

Fig. 7. Effect of ZD6474 (▽, 25 mg/kg/day; △, 50 mg/kg/day;○, 100 mg/kg/day) or vehicle (■) on the growth of syngeneic tumor models [*a*, B16-F10(AP3) melanoma; *b*, Lewis Lung carcinoma]. Tumor cells were implanted s.c. in the flank of immunocompetent C57/BL6 mice. Once-daily oral administration of ZD6474 or vehicle was started from the day of tumor cell implantation and continued for the duration of the experiment. Data points represent a mean from 10 mice, with SEs shown in one direction.

Fig. 8. Analysis of ZD6474-treated Calu-6 tumor xenografts ($n = 5$). a, histological sections (×1.6 objective) of (i) control (vehicle-treated) and (ii) ZD6474 (50 mg/kg/day)-treated Calu-6 tumors stained for CD31. Tumors were established (0.16 cm³) before 24 days of continuous therapy. A significant reduction in CD31 (endothelial cell) staining was evident after ZD6474 treatment. Mean CD31-positive area/5000 μm² viable tumor (b) and percentage of total tumor necrosis (c), as determined by morphometric image analysis after 24 days of treatment with vehicle or ZD6474 (25–100 mg/kg/day, once daily, p.o.), are shown. *, $P \le 0.001$ by one-tailed t test.
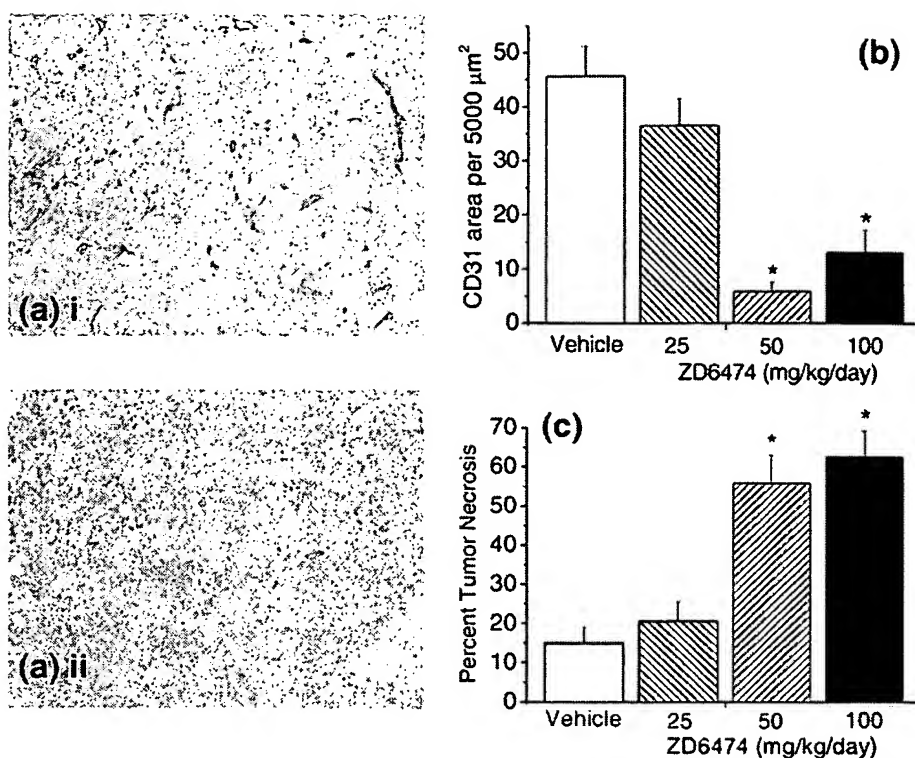
not share the same broad spectrum of activity in the panel of tumor xenografts examined in this study (data not shown). For example, the activity of ZD6474 has been compared with a selective EGFR TKI, after administration of 50 mg/kg/day of either compound (p.o., 21 days) to mice bearing the EGFR-overexpressing vulval tumor A431 or the PC-3 prostate tumor. Whereas ZD6474 produced substantial inhibition of tumor growth in both tumors ($\ge 87\%$; $P < 0.001$), the EGFR TKI produced a highly significant inhibition in the EGFR-overexpressing tumor A431 (94%; $P < 0.001$) but did not significantly affect the growth of PC-3 ($P > 0.1$). Subsequent experiments examining selective VEGFR TKIs have also demonstrated that activity versus KDR alone is sufficient to exert significant antitumor activity in the Calu-6 lung tumor xenograft (71). Hence, the antitumor activity of ZD6474 may extend to a wide range of solid tumor types by virtue of its ability to inhibit VEGF signal transduction.

Given that inhibition of VEGF signaling was required for activity in the PC-3 tumor model, it is perhaps surprising that well-established PC-3 tumor xenografts were observed to regress dramatically when treated with ZD6474. This was not apparent in well-established Calu-6 tumors; however, encouragingly, highly significant inhibition of tumor growth was observed in this model, irrespective of the tumor volume at start of ZD6474 treatment. The divergent responses observed in these tumor models may reflect different dependencies on VEGF as a survival factor for newly formed endothelium (7, 72). Such signaling is known to involve Akt/protein kinase B activation and has been suggested to depend on formation of a multimeric complex between the cytoplasmic domains of KDR, the endothelial adherens junction molecule VE-cadherin, β-catenin, and phophoinositide 3-kinase (8).

In summary, we have identified ZD6474, a potent nanomolar inhibitor of VEGF signaling with pharmacokinetic properties compatible with chronic oral administration. This compound is also a submicromolar inhibitor of EGFR tyrosine kinase, which, at higher doses, may offer added therapeutic benefit in tumors with EGFR-dependent
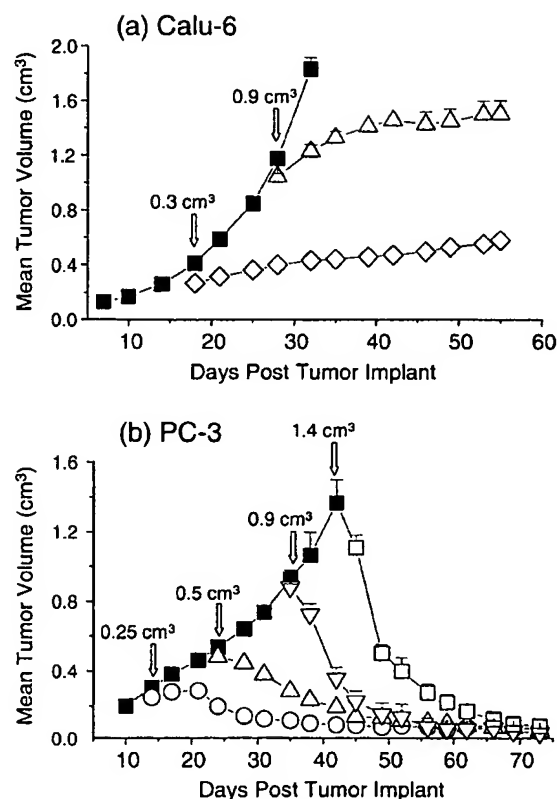

Fig. 9. Effect of ZD6474 on well-established human tumor xenografts. Mice bearing s.c. human tumors were divided into groups with different mean volumes as tumor growth advanced (0.15–1.4 cm³) and then chronically treated with ZD6474 (100 mg/kg/day, p.o.). Arrows indicate the start of ZD6474 treatment (a, Calu-6; b, PC-3). Data points represent the means for 10 mice, with SE bars shown in one direction. a, comparable inhibition of tumor growth was induced in Calu-6 tumors of 0.3 or 0.9 cm³ volume. b, ZD6474 induced regression in all PC-3 tumors.

proliferation or survival. ZD6474 is currently in Phase 1 clinical development as a once-daily oral therapy for the treatment of cancer (73).

REFERENCES

1. Keck, P. J., Hauser, S. D., Krivi, G., Sanzo, K., Warren, T., Feder, J., and Connolly, D. T. Vascular permeability factor, an endothelial cell mitogen related to PDGF. Science (Wash. DC), 246: 1309–1312, 1989.
2. Lamoreaux, W. J., Fitzgerald, M. E., Reiner, A., Hasty, K. A., and Charles, S. T. Vascular endothelial growth factor increases release of gelatinase A and decreases release of tissue inhibitor of metalloproteinases by microvascular endothelial cells in vitro. Microvasc. Res., 55: 29–42, 1998.
3. Pepper, M. S., Montesano, R., Mandroita, S. J., Orci, L., and Vassalli, J. D. Angiogenesis: a paradigm for balanced extracellular proteolysis during cell migration and morphogenesis. Enzyme Protein, 49: 138–162, 1996.
4. Asahara, T., Murohara, T., Sullivan, A., Silver, M., van der Zee, R., Li, T., Witzenbichler, B., Schatteman, G., and Isner, J. M. Isolation of putative progenitor endothelial cells for angiogenesis. Science (Wash. DC), 275: 964–967, 1997.
5. Gehling, U. M., Ergün, S., Schumacher, U., Wagener, C., Pantel, K., Otte, M., Schuch, G., Schafhausen, P., Mende, T., Kilic, N., Kluge, K., Schäfer, B., Hossfeld, D. K., and Fiedler, W. In vitro differentiation of endothelial cells from AC133-positive progenitor cells. Blood, 95: 3106–3112, 2000.
6. Gargett, C. E., Lederman, F., Heryanto, B., Gambino, L. S., and Rogers, P. A. W. Focal vascular endothelial growth factor correlates with angiogenesis in human endometrium. Role of intravascular neutrophils. Hum. Reprod., 16: 1065–1075, 2001.
7. Benjamin, L. E., Golijanin, D., Itin, A., Pode, D., and Keshet, E. Selective ablation of immature blood vessels in established human tumours follows vascular endothelial growth factor withdrawal. J. Clin. Invest., 103: 159–165, 1999.
8. Carmeliet, P., Lampugnani, M. G., Moons, L., Breviario, F., Compernolle, V., Bono, F., Balconi, G., Spagnuolo, R., Oostuyse, B., Dewerchin, M., Zanetti, A., Angellilo, A., Mattot, V., Nuyens, D., Lutgens, E., Clotman, F., de Ruiter, M. C., Gittenberger-de Groot, A., Poelmann, R., Lupu, F., Herbert, J. M., Collen, D., and Dejana, E. Targeted deficiency or cytosolic truncation of the VE-cadherin gene in mice impairs VEGF-mediated endothelial survival and angiogenesis. Cell, 98: 147–157, 1999.
9. Benjamin, L. E., Hemo, I., and Keshet, E. A plasticity window for blood vessel remodelling is defined by pericyte coverage of the preformed endothelial network and is regulated by PDGF-B and VEGF. Development (Camb.), 125: 1591–1598, 1998.
10. Yamagishi, S., Yonekura, H., Yamamoto, Y., Fujimori, H., Sakurai, S., Tanaka, N., and Yamamoto, H. Vascular endothelial growth factor acts as a pericyte mitogen under hypoxic conditions. Lab. Invest., 79: 501–509, 1999.
11. Dvorak, H. F., Detmar, M., Claffey, K. P., Nagy, J. A., van de Water, L., and Senger, D. R. Vascular permeability factor/vascular endothelial growth factor: an important mediator of angiogenesis in malignancy and inflammation. Int. Arch. Allergy Immunol., 107: 233–235, 1995.
12. Bates, D. O., Heald, R. I., Curry, F. E., and Williams, B. Vascular endothelial growth factor increases Rana vascular permeability and compliance by different signalling pathways. J. Physiol. (Lond.), 533: 263–272, 2001.
13. Carmeliet, P., and Jain, R. K. Angiogenesis in cancer and other diseases. Nature (Lond.), 407: 249–257, 2000.
14. Folkman, J. Angiogenesis in cancer, vascular, rheumatoid and other disease. Nat. Med., 1: 27–31, 1995.
15. Plendl, J. Angiogenesis and vascular regression in the ovary. Anat. Histol. Embryol., 29: 257–266, 2000.
16. Howdieshell, T. R., Callaway, D., Webb, W. L., Gaines, M. D., Procter, C. D., Jr., Sathyanarayana, J. S. Pollock, J. S., Brock. T. L., and McNeil, P. L. Antibody neutralization of vascular endothelial growth factor inhibits wound granulation tissue formation. J. Surg. Res., 96: 173–182, 2001.
17. Asahara, T., Chen, D., Takahashi, T., Fujikawa, K., Kearney, M., Magner, M., Yancopoulos, G. D., and Isner, J. M. Tie2 receptor ligands, angiopoietin-1 and angiopoietin-2, modulate VEGF-induced postnatal neovascularisation. Circ. Res., 83: 233–240, 1998.
18. Shin, D., Garcia-Cardena, G., Hayashi, S., Gerety, S., Asahara, T., Stavrakis, G., Isner, J., Folkman, J., Gimbrone. M. A., Jr., and Andreson, D. J. Expression of ephrinB2 identifies a stable genetic difference between arterial and venous vascular smooth muscle as well as endothelial cells, and marks subsets of microvessels at sites of adult neovascularisation. Dev. Biol., 230: 139–150, 2001.
19. Plate, K. H., Breier, G., Weich. H. A., Mennel, H. D., and Risau, W. Vascular endothelial growth factor and glioma angiogenesis: coordinate induction of VEGF receptors, distribution of VEGF protein and possible in vivo regulatory mechanisms. Int. J. Cancer, 59: 520–529, 1994.
20. Damert, A., Ikeda, E., and Risau, W. Activator-protein-1 binding potentiates the hypoxia-inducible factor-1-mediated hypoxia-induced transcriptional activation of vascular-endothelial growth factor expression in C6 glioma cells. Biochem. J., 327: 419–423, 1997.
21. Dibbens, J. A., Miller, D. L., Damert, A., Risau, W., Vadas, M. A., and Goodall, G. J. Hypoxic regulation of vascular endothelial growth factor mRNA stability requires the cooperation of multiple RNA elements. Mol. Biol. Cell, 10: 907–919, 1999.
22. Zhang, L., Yu, D., Hu, M., Xiong, S., Lang, A., Ellis, L. M., and Pollock, R. E. Wild-type p53 suppresses angiogenesis in human leiomyosarcoma and synovial sarcoma by transcriptional suppression of vascular endothelial growth factor expression. Cancer Res., 60: 3655–3661, 2000.
23. Mukhopadhyay, D., Knebelmann, B., Cohen, H. T., Anath, S., and Sukhatme. V. P. The von Hippel-Lindau tumor suppressor gene product interacts with Sp1 to repress vascular endothelial growth factor promoter activity. Mol. Cell. Biol., 17: 5629–5639, 1997.
24. Rak, J., Mitsuhashi, L., Bayo, L., Filmus, J., Shirasawa, S., Sasazuki, T., and Kerbel, R. S. Mutant ras oncogenes up-regulate VEGF/VPF expression: implications for induction and inhibition of tumor angiogenesis. Cancer Res., 55: 4575–4580, 1995.
25. Ellis, L. M., Staley, C. A., Liu, W., Fleming. R. Y., Parikh. N. U., Bucana, C. D., and Gallick, G. E. Down-regulation of vascular-endothelial growth factor in a human colon carcinoma cell line transfected with an antisense expression vector specific for c-src. J. Biol. Chem., 273: 1052–1057, 1998.
26. Robinson, D. R., Wu, Y-M., and Lin, S-F. The protein tyrosine kinase family of the human genome. Oncogene, 19: 5548–5557, 2000.
27. Petrova. T., Makinen, T., and Alitalo, K. Signaling via vascular endothelial growth factor receptors. Exp. Cell Res., 253: 117–130, 1999.
28. Kaipainen, A., Korhonen, J., Mustonen, T., van Hinsbergh, V. W., Fang, G. H., Dumont, D., Breitman, M., and Alitalo, K. Expression of the fms-like tyrosine kinase 4 gene becomes restricted to lymphatic endothelium during development. Proc. Natl. Acad. Sci. USA, 92: 3566–3570, 1995.
29. Joukov, V., Pajusola, K., Kaipainen, A., Chilov, D., Lahtinen, I., Kukk, E., Saksela, O., Kalkkinen, N., and Alitalo, K. A novel vascular endothelial growth factor, VEGF-C, is a ligand for the Flt-4 (VEGFR-3) and KDR (VEGFR-2) receptor tyrosine kinases. EMBO J., 15: 290–298, 1996.
30. Achen, M. G., Jeltsch, M., Kukk, E., Makinen, T., Vitali, A., Wilks, A. F., Alitalo, K., and Stacker. S. A. Vascular endothelial growth factor D (VEGF-D) is a ligand for the tyrosine kinases VEGF receptor 2 (Flk1) and VEGF receptor 3 (Flt4). Proc. Natl. Acad. Sci. USA, 95: 548–553, 1998.
31. Huang, K., Andersson. C., Roomans, G. M., Ito, N., and Claesson-Welsh, L. Signaling properties of VEGF receptor-1 and -2 homo- and heterodimers. Int. J. Biochem. Cell Biol., 33: 315–324, 2001.
32. Whitaker, G. B., Limberg, B. J., and Rosenbaum, J. S. Vascular endothelial growth factor receptor-2 and neuropilin-1 form a receptor complex that is responsible for the differential signalling potency of $VEGF_{165}$ and $VEGF_{121}$. J. Biol. Chem., 276: 25520–25531, 2001.
33. Gluzman-Poltorak, Z., Cohen, T., Shibuya, M., and Neufeld, G. Vascular endothelial growth factor receptor-1 and neuropilin-2 form complexes. J. Biol. Chem., 276: 18688–18694, 2001.
34. Bachelder, R. E., Crago, A., Chung, J., Wendt, M. A., Shaw, L. M., Robinson, G., and Mercurio, A. M. Vascular endothelial growth factor is an autocrine survival factor for neuropilin-expressing breast carcinoma cells. Cancer Res., 61: 5736–5740, 2001.
35. Meyer, M., Clauss, M., Lepple-Wienhues, A., Waltenberger, J., Augustin, H. G., Ziche, M., Lanz, C., Büttner, M., Rziha, H-J., and Dehio, C. A novel vascular endothelial growth factor encoded by Orf virus, VEGF-E, mediates angiogenesis via signalling through VEGFR-2 (KDR) but not VEGFR-1 (Flt-1) receptor tyrosine kinase. EMBO J., 18: 363–374, 1999.
36. Zeng, H., Sanyal, S., and Mukhopadhyay, D. Tyrosine residues 951 and 1059 of vascular endothelial growth factor receptor-2 (KDR) are essential for vascular permeability factor/vascular endothelial growth factor-induced endothelium migration and proliferation, respectively. J. Biol. Chem., 276: 32714–32719, 2001.
37. Gille, H., Kowalski, J., Li, B., LeCouter, J., Moffat, B., Zioncheck, T. F., Pelletier, N., and Ferrara, N. Analysis of biological effects and signalling properties of Flt-1 (VEGFR-1) and KDR (VEGFR-2). J. Biol. Chem., 276: 3222–3230, 2001.
38. Gordon, M. S., Margolin, K., Talpaz, M., Sledge, G. W., Holmgren, E., Benjamin, R., Stalter, S., Shak, S., and Adelman, D. Phase I safety and pharmacokinetic study of recombinant human anti-vascular endothelial growth factor in patients with advanced cancer. J. Clin. Oncol., 19: 843–850, 2001.
39. Hunt, S. Technology evaluation: IMC-1C11. ImClone Systems. Curr. Opin. Mol. Ther., 3: 418–424, 2001.
40. Wedge, S. R., Ogilvie, D. J., Dukes, M., Kendrew, J., Curwen, J. O., Hennequin, L. F., Thomas, A. P., Stokes, E. S. E., Curry, B., Richmond, G. H. P., and Wadsworth, P. ZD4190: an orally active inhibitor of vascular endothelial growth factor signaling with broad-spectrum antitumor efficacy. Cancer Res., 60: 970–975, 2000.
41. Hennequin, L. F., Stokes, E. S. E., Thomas, A. P., Johnstone. C., Plé, P. A., Ogilvie, D. J., Dukes, M., Wedge, S. R., Kendrew, J., and Curwen. J. O. Novel 4-anilino-quinazolines with C-7 basic side chains. Design and structure activity relationship of a series of potent, orally active. VEGF receptor tyrosine kinase inhibitors. J. Med. Chem., 45: 1300–1312, 2002.
42. Hennequin, L. F., Thomas, A. P., Johnstone, C., Stokes, E. S. E., Plé, P. A., Lohmann, J. M., Ogilvie, D. J., Dukes, M., Wedge, S. R., Curwen, J. O., Kendrew, J., and Lambert-van der Brempt, C. Design and structure-activity relationship of a new class of potent VEGF receptor tyrosine kinase inhibitors. J. Med. Chem., 42: 5369–5389, 1999.

43. Curwen, J. O., and Ogilvie, D. J. Production of the angiogenic factors VEGF and bFGF at tumour sites may also confer an acute haemodynamic advantage to the tumour. Br. J. Cancer, 75 (Suppl. 1): P89, 1997.

44. Kreisle, R. A., and Ershler. W. B. Investigation of tumor angiogenesis in an id mouse model: role of host tumor interactions. J. Natl. Cancer Inst. (Bethesda), 26: 849–854, 1988.

45. Auerbach, R., Auerbach. W., and Polakowski. I. Assays for angiogenesis: a review. Pharmacol. Ther., 51: 1–11, 1991.

46. Lopez, J. J., Laham, R. J., Carrozza, J. P., Tofukuji, M., Sellke, F. W., Bunting, S., and Simons, M. Hemodynamic effects of intracoronary VEGF delivery: evidence of tachyphylaxis and NO dependence of response. Am. J. Physiol., 273: H1317–H1323, 1997.

47. Horner, A., Bishop, N. J., Bord. S., Beeton, C., Kelsall, A. W., Coleman, N., and Compston, J. E. Immunolocalisation of vascular endothelial growth factor (VEGF) in human neonatal growth plate cartilage. J. Anat., 194: 519–524, 1999.

48. Waltenberger, J., Claesson-Welsh, L., Siegbahn, A., Shibuya, M., and Heldin. C-H. Different signal transduction properties of KDR and Flt-1: two receptors for vascular endothelial growth factor. J. Biol. Chem., 269: 26988–26995, 1994.

49. Kroll, J., and Waltenberger, J. The vascular endothelial growth factor receptor KDR activates multiple signal transduction pathways in porcine aortic endothelial cells. J. Biol. Chem., 272: 32521–32527, 1997.

50. Hiratsuka, S., Minowa, O., Kuno, J., Noda, T., and Shibuya, M. Flt-1 lacking the tyrosine kinase domain is sufficient for normal development and angiogenesis in mice. Proc. Natl. Acad. Sci. USA, 95: 9349–9354, 1998.

51. Carmeliet, P., Moons, L., Luttun, A., Vincenti, V., Compernolle. V., De Mol, M., Wu, Y., Bono, F., Devy. L., Beck. H., Scholtz, D., Acker, T., DiPalma, T., Dewerchin. M., Noel, A., Stalmans. I., Barra, A., Blacher, S., Vandendriessche. T., Ponten, A., Eriksson, U., Plate, K. H., Foidart, J. M., Schaper, W., Charnock-Jones, D. S., Hicklin. D. J., Herbert, J. M., Collen, D., and Persico, M. G. Synergism between vascular endothelial growth factor and placental growth factor contributes to angiogenesis and plasma extravasation in pathological conditions. Nat. Med., 7: 575–583, 2001.

52. Valtola, R., Salven. P., Heikkila, P., Taipale, J., Joensuu, H., Rehn, M., Pihlajaniemi, T., Weich, H., de Waal, R., and Alitalo, K. VEGFR-3 and its ligand VEGF-C are associated with angiogenesis in breast cancer. Am. J. Pathol., 154: 1381–1390, 1999.

53. Partanen, T. A., Alitalo, K., and Miettinen, M. Lack of lymphatic vascular specificity of vascular endothelial growth factor receptor 3 in 185 vascular tumors. Cancer (Phila.), 86: 2406–2412, 1999.

54. Kinoshita, J., Kitamura, K., Kabashima, A., Saeki, H., Tanaka, S., and Sugimachi, K. Clinical significance of vascular endothelial growth factor-C (VEGF-C) in breast cancer. Breast Cancer Res. Treat., 66: 159–164, 2001.

55. Ichikura, T., Tomimatsu, S., Ohkura, E., and Mochizuki, H. Prognostic significance of the expression of vascular endothelial growth factor (VEGF) and VEGF-C in gastric carcinoma. J. Surg. Oncol., 78: 132–137, 2001.

56. Morbidelli, L., Chang, C. H., Douglas, J. G., Granger, H. J., Ledda, F., and Ziche, M. Nitric oxide mediates mitogenic effect of VEGF on coronary venular endothelium. Am. J. Physiol., 270: H411–H415, 1996.

57. Wu, H. M., Yuan, Y., McCarthy, M., and Granger, H. J. Acidic and basic FGFs dilate arterioles of skeletal muscle through a NO-dependent mechanism. Am. J. Physiol., 271: H1087–H1093, 1996.

58. Gerber, H-P., and Ferrara, N. Angiogenesis and bone growth. Trends Cardiovasc. Med., 10: 223–228, 2000.

59. Gerber, H-P., Vu, T. H., Ryan, A. M., Kowalski, J., Werb, Z., and Ferrara, N. VEGF couples hypertrophic cartilage remodeling, ossification and angiogenesis during endochondral bone formation. Nat. Med., 5: 623–628, 1999.

60. Haigh, J. J., Gerber, H-P., Ferrara N., and Wagner, E. F. Conditional inactivation of VEGF-A in areas of collagen2a1 expression results in embryonic lethality in the heterozygous state. Development (Camb.), 127: 1445–1453, 2000.

61. Woodburn, J. R. The epidermal growth factor receptor and its inhibition in cancer therapy. Pharmacol. Ther., 82: 241–250, 1999.

62. Salomon, D. S., Brandt, R., Ciardello, F., and Normanno, N. Epidermal growth factor-related peptides and their receptors in human malignancies. Crit. Rev. Oncol. Hematol., 19: 183–232, 1995.

63. Musallam, L., Ethier, C., Haddad, P. S., and Bilodeau, M. Role of EGF receptor tyrosine kinase activity in antiapoptotic effect of EGF on mouse hepatocytes. Am. J. Physiol. Gastrointest. Liver Physiol., 280: G1360–G1369, 2001.

64. Alper, O., Bergmann-Leitner, E. S., Bennett, T. A., Hacker, N. F., Stromberg, K., and Stetler-Stevenson, W. G. Epidermal growth factor receptor signalling and the invasive phenotype of ovarian carcinoma cells. J. Natl. Cancer Inst. (Bethesda), 19: 1375–1384, 2001.

65. Ciardiello, F., Caputo, R., Bianco, R., Damiano, V., Fentanini, G., Cuccato, S., De Placido, S., Bianco, A. R., and Tortora, G. Inhibition of growth factor production and angiogenesis in human cancer cells by ZD1839 (Iressa), a selective epidermal growth factor receptor tyrosine kinase inhibitor. Clin. Cancer Res., 7: 1459–1465, 2001.

66. Baselga, J., Pfister, M. R., Cooper, M. R., Cohen, R., Burtness, B., Bos, M., D'Andrea, G., Seidman, A., Norton, L., Gunnett. K., Falcey, J., Anderson, V., Waksal, H., and Mendelsohn, J. Phase I studies of anti-epidermal growth factor receptor chimeric antibody C225 alone and in combination with cisplatin. J. Clin. Oncol., 18: 904–914, 2000.

67. Ciardiello, F. Epidermal growth factor receptor tyrosine kinase inhibitors as anticancer agents. Drugs, 60 (Suppl. 1): 25–32, 2000.

68. Krensel, K., and Lichtner, R. B. Selective increase of α2-integrin sub-unit expression on human carcinoma cells upon EGF-receptor activation. Int. J. Cancer, 80: 546–552, 1999.

69. Petit, A. M., Rak, J., Hung, M. C., Rockwell, P., Goldstein, N., Fendly, B., and Kerbel, R. S. Neutralizing antibodies against epidermal growth factor and ErbB-2/neu receptor tyrosine kinases down-regulate vascular endothelial growth factor production by tumor cells in vitro and in vivo: angiogenic implications for signal transduction therapy of solid tumors. Am. J. Pathol., 151: 1523–1530, 1997.

70. Shaheen, R. M., Ahmad, S. A., Liu, W., Reinmuth, N., Jung, Y. D., Tseng, W. W., Drazan, K. E., Bucana, C. D., Hicklin, D. J., and Ellis, L. M. Inhibited growth of colon cancer carcinomatosis by antibodies to vascular endothelial and epidermal growth factor receptors. Br. J. Cancer, 85: 584–589, 2001.

71. Hennequin, L. F., Stokes, E. S. E., McKerrecher, D., Plé, P., Ogilvie, D. J., Dukes, M., Wedge, S. R., and Kendrew, J. Structure activity relationship and in vivo efficacy of indole-quinazolines, a novel series of selective and orally active inhibitors of VEGF receptor tyrosine kinase activity (Flt-1 and KDR). Proc. Am. Assoc. Cancer Res., 42: 584, 2001.

72. Alon, T., Hemo, I., Itin, A., Pe'ee, J., Stone, J., and Keshet, E. Vascular endothelial factor acts as a survival factor for newly formed retinal vessels and has implications for retinopathy of prematurity. Nat. Med., 1: 1024–1028, 1995.

73. Basser, R., Hurwitz, H., Barge, A., Davis, I., DeBoer, R., Holden, S. N., McArthur, G., McKinley, M., Nairn, K., Persky, M., Rischin, D., Rosenthal, M., Swaisland, H., and Eckhardt, S. G. Phase I pharmacokinetic and biological study of the angiogenesis inhibitor, ZD6474, in patients with solid tumors. Proc. Am. Soc. Clin. Oncol., 37: 21, 2001.